# ChemComm

Chemical Communications

www.rsc.org/chemcomm

Number 38 | 14 October 2008 | Pages 4509–4648

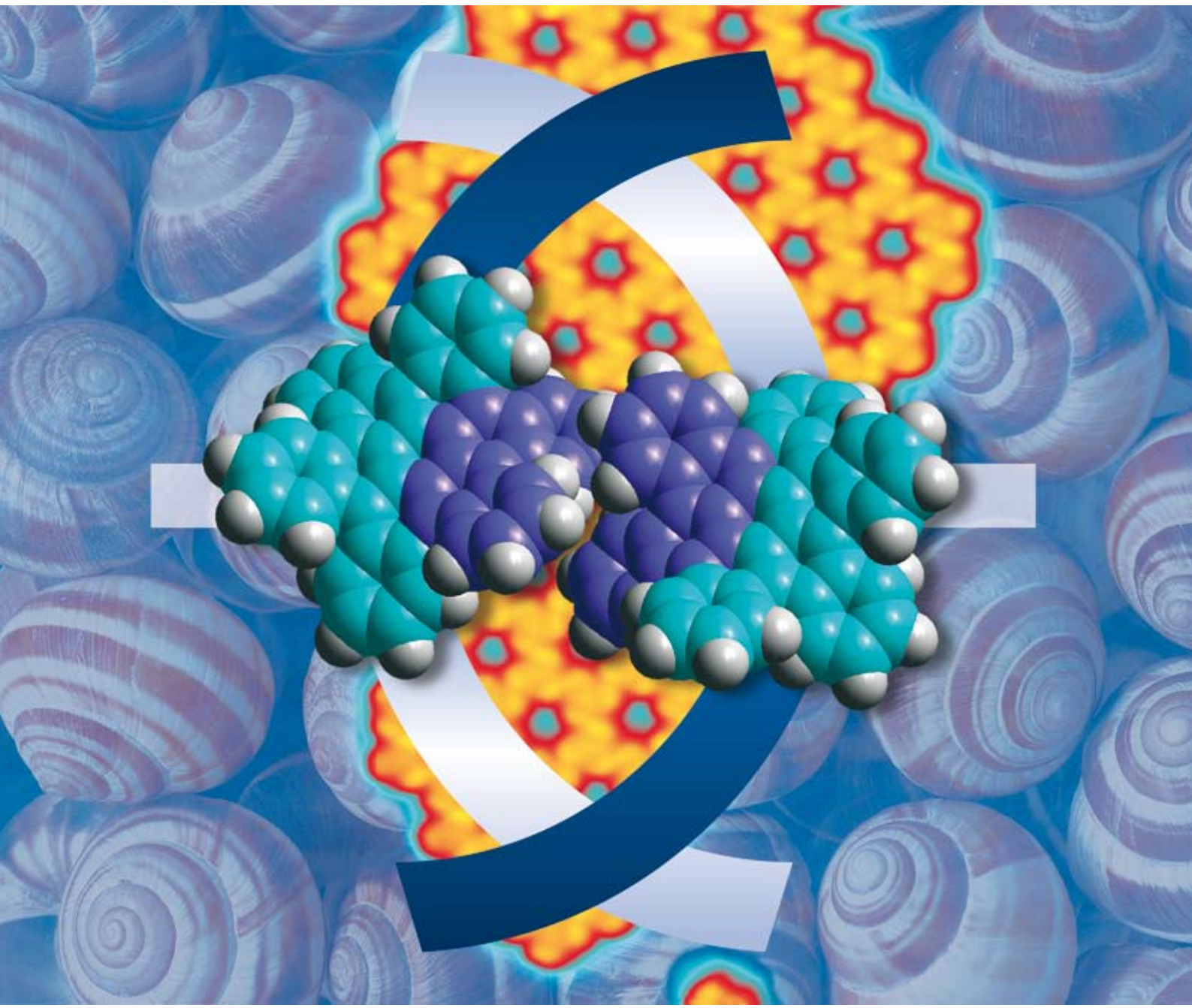

ISSN 1359-7345



RSC Publishing

# An aromatic coupling motif for two-dimensional supramolecular architectures†

**Matthias Treier,*[a] Pascal Ruffieux,[a] Pierangelo Gröning,[a] Shengxiong Xiao,[b] Colin Nuckolls[b] and Roman Fasel[a]**

*Received (in Cambridge, UK) 6th June 2008, Accepted 11th August 2008*
*First published as an Advance Article on the web 27th August 2008*
**DOI: 10.1039/b809618j**

**We show, using scanning tunneling microscopy, how a coupling motif based on self-complementary helical aromatic units is able to drive the formation of a chiral porous supramolecular network and chains based on lateral aromatic interactions in two dimensions.**

Self-assembly is a promising concept for the nanoscale fabrication of future molecular electronic devices[1] allowing for 'automatic' bottom-up production guided by the design of the molecular building blocks and the underlying substrate surface.[2] Molecules containing polycyclic aromatic units are among the most promising candidates for such applications because of the comparably high charge carrier mobilities that can be achieved.[3] By adapting the principles of supramolecular chemistry to the two-dimensional (2D) case, supramolecular nanostructures of such molecules have been realized on single crystal surfaces by hydrogen bonding[4] and metal-coordination.[5] However, these types of bonds are generally non-conducting, which prevents nanoelectronic applications. We report on a lateral coupling motif which has the potential to overcome this problem by the use of aromatic interactions. This coupling motif, consisting of two self-complementary helical aromatic units, is capable of driving the formation of 2D supramolecular structures and holds promise for organizing charge carrier pathways.

Submonolayer coverage self-assembly of the non-planar polycyclic aromatic hydrocarbon (PAH) hexa-*cata*-hexabenzocoronene (HBC)[6] (Fig. 1) on Cu(111) has been investigated by scanning tunneling microscopy (STM). Sample preparation and measurements were conducted in an ultra high vacuum system with a base pressure below $2 \times 10^{-10}$ mbar using an Omicron low temperature STM. The Cu(111) substrate was cleaned by repeated cycles of $Ar^+$ ion sputtering and subsequent annealing to 750 K. HBC has been deposited on the clean single crystal surface under ultra high vacuum at a rate of approximately 0.1 ML $min^{-1}$ from resistively heated quartz crucibles at 560 K. During deposition, the sample was kept at room temperature and subsequently cooled down to 77 K for STM analysis.

At submonolayer HBC coverage, large islands of a porous network are formed, where each hole is surrounded by six HBC molecules (Fig. 1a). Neighboring molecules are rotated by 180° with respect to each other, such that upwards-/downwards-facing neighboring aromatic rings of one HBC molecule are pointing towards a downwards-/upwards-facing pair of rings of the neighboring molecule. The lateral binding motif consists of two interdigitated self-complementary helical aromatic units facing (and partially interlocked with) each other.

The same coupling motif can also lead to linear supramolecular chains (Fig. 1b) that show the same intermolecular distance and identical molecular orientation with respect to the substrate. The orientation of the adsorbate with respect to the Cu substrate is typical for adsorption of PAHs on this substrate, with acene units being aligned with close-packed directions of the substrate.[7] Partial overlap between π-electron systems of neighboring molecules makes the linear structures

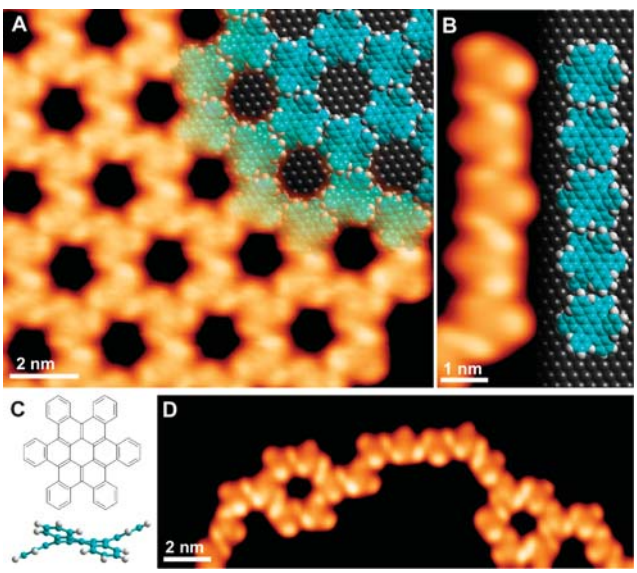


**Fig. 1** (a) STM image‡ (−1.8 V, 30 pA) of a supramolecular HBC honeycomb network with 2.3 nm pore-to-pore distance and molecular model. (b) STM image (−1.9 V, 20 pA) and model of linear chain formed through the same coupling motif. (c) Chemical structure of HBC. The side view visualizes the non-planarity of the aromatic system. (d) STM image (−2.1 V, 50 pA) of interconnected linear strands and honeycomb structures of opposite chirality.

[a] *Empa, Swiss Federal Laboratories for Materials Testing and Research, nanotech@surfaces laboratory, Feuerwerkerstrasse 39, 3602 Thun, Switzerland. E-mail: matthias.treier@empa.ch; Fax: +41 33 228 44 90; Tel: +41 33 228 22 37*
[b] *Columbia University, Department of Chemistry, Havemeyer Mail Code 3130, 3000 Broadway, New York, NY 10027, USA*
†Electronic supplementary information (ESI) available: Experimental data (large scale STM images and manipulation of polymolecular units) and definition of tetrahelicene units. See DOI: 10.1039/b809618j

potential nanowire-like conductors. The orbital overlap results in a splitting of the HOMO/LUMO levels which gives rise to an increased mobility for holes/electrons.[8] These linear structures are observed growing out from step edges of the underlying substrate surface or as connections between honeycomb structures as shown in Fig. 1d.

For a given peripheral carbon ring, two mirror-symmetric enantiomers of the helical units can be defined (*M*- and *P*-tetrahelicene, see ESI for details†) leading to two inequivalent coupling directions and hence, to two chiral domains of the honeycomb network (Fig. 2a). Both domains are experimentally observed and correspond to commensurate 9 × 9 superstructures, with two molecules per unit cell. Lateral coupling *via* the *M*-tetrahelicene units gives rise to "left-handed" λ-domains of the honeycomb network, whereas "right-handed" ρ-domains consist of HBC molecules coupled *via* their *P*-tetrahelicene units (see Fig. 2b). It should be noted, that honeycombs are enantiopure (in the coupling motif) whereas linear strands correspond to enantiomeric mixtures of *M*–*M* and *P*–*P*-coupled units.

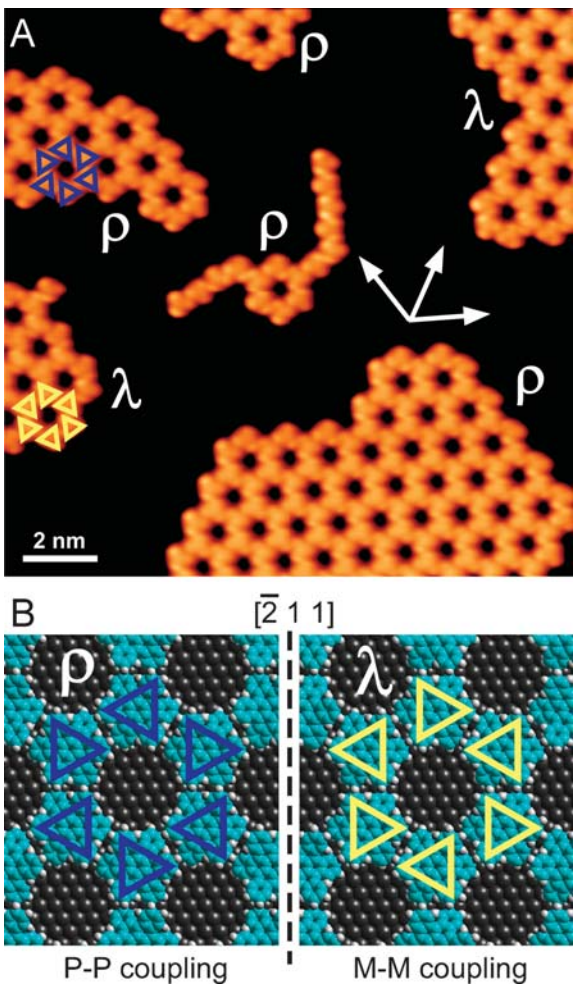


**Fig. 2** (a) STM image (−1.9 V, 20 pA) showing the two chiral domains of the honeycomb network. The arrows indicate the orientation of the close-packed directions of the substrate. (b) Models for the ρ and λ honeycomb domains. The coloured triangles visualize the orientation of the adsorbates, with corners lying over upwards facing rings of HBC.

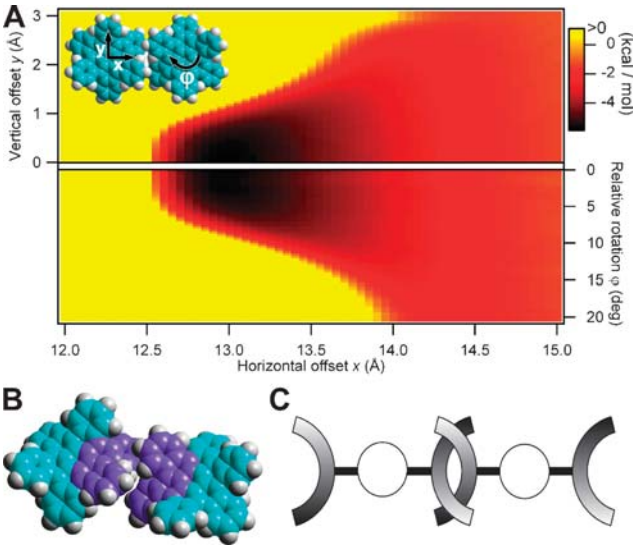


**Fig. 3** (a) Interaction energy for two HBC molecules in the interdigitated helical aromatic units recognition geometry as a function of relative position and orientation. The upper/lower halves of the plot are relative to the left/right axes, respectively. The color scale shows the interaction energy in kcal $mol^{-1}$, with yellow corresponding to repulsive interaction. (b) Coupling motif driving supramolecular organization: Self-complementary helical aromatic units (violet) interdigitate and lock in place by aromatic interactions. (c) Schematic representation of the helical aromatic coupling unit and its incorporation in arbitrary supramolecular structures.

It can be seen that the lateral distance and respective orientation of nearest neighbors is identical in all three different structures, proving that they rely on the same lateral binding motif. Unlike the linear structures that grow from step edges, honeycomb networks are found at the centre of substrate terraces and do not extend up to the step edges surrounding these terraces. The honeycomb structures are more frequently observed than their linear counterparts. Apart from molecules decorating substrate defect sites (*e.g.* step edges) no individual molecules are found on the terraces, indicating a high molecular mobility at the deposition temperature.

The interaction energy of two HBC molecules in the interdigitated helical aromatic units recognition geometry has been computed as a function of relative molecular position and orientation by molecular mechanics calculations (see Fig. 3a).§ The color plot visualizes the shallow potential minimum for displacements along the coupling direction (*x*-axis) and the directionality of the coupling motif. It can be seen that due to steric hindrance between shifted (left axis) or rotated (right axis) helical units, lateral out-of-registry displacements and rotations are limited to less than 1 Å and a few degrees, respectively. Steric hindrance between hydrogen atoms of neighbouring adsorbates bestows to this coupling motif a strong orientational stability beyond the one expected for aromatic interactions between completely planar aromatic systems. The absolute minimum of the interaction potential is located at a center-to-center distance of 13.0 Å (at 0° relative rotation) which compares well with the experimentally observed distance of 13.3 Å (for both honeycombs and chains).

This shallow interaction potential will allow for a commensurate registry with various substrates as the energetic cost for variations in bonding distance is low. This is in line with the well-known versatility of aromatic interactions compared to stronger noncovalent bonds, which allows for a large range of energetically favorable bond lengths and angles as inferred for example by studies on aromatic interactions in proteins.[11]

The effective contact surface of the interdigitated tetrahelicene units is small compared to systems with strongly interdigitating units such as alkyl chains that are frequently used to stabilize solution-based 2D supramolecular architectures.[12] However, molecules containing several long alkyl chains can often not be sublimated intact, preventing studies under UHV conditions. The coupling motif which is here used for two-dimensional architectures might in principle also be applied for supramolecular architectures in three dimensions. However, in the absence of geometrical constraints, the interlocked helical units geometry might not be energetically favoured over other geometries in which the total overlap of aromatic subunits is maximized.

The possibility of small adsorption-induced conformational changes has also been investigated with molecular mechanics simulations. Changes in conformation would involve a collective upwards/downwards bending of the outermost molecular units. This would imply a change in the bending angle of the acene units. Calculations show that no important conformational changes can be expected in the adsorbed state since changes in bending angle by more than approximately 4° result in a significant increase in strain energy. The aromatic interaction between nearest neighbors has also been calculated for these conformations. Both the shape and total energy of the interaction potential remain unaffected by small conformational changes. This shows that the binding motif (Fig. 3b) is inherently rigid and remains unaffected by possible small adsorption-induced conformational changes, which is important as the conformation of large molecules in the adsorbed state is difficult to predict. Previous studies on the self-assembly of rubrene and calix[4]arenes on single crystal surfaces[13] have shown that aromatic interactions can play a major role in stabilizing two-dimensional supramolecular structures on single crystal surfaces. However, the conformational flexibility of the aromatic units of these molecules hinders the prediction of supramolecular structures of such molecules on different substrates, preventing a clear isolation of the coupling motifs. The inherently rigid aromatic coupling motif presented in this *communication* overcomes this problem, making aromatically bonded supramolecular structures more predictable. This coupling motif is not limited to work only on Cu(111) but should also be applicable to any other substrates on which adsorbate–substrate interactions only exhibit a weak lateral modulation.

In this work we have shown—using a non-planar PAH which incorporates self-complementary helical aromatic units—that surface-supported two-dimensional supramolecular architectures can be realized through lateral aromatic interactions. Interdigitated helical aromatic coupling motifs may be used with other molecular building blocks to grow tailor-made structures with overlapping π-electron systems (see schematic model in Fig. 3c). The aromatic interactions' ability to relax to characteristic substrate distances, combined with a careful patterning of the substrate surface presents a means to tailor structures for molecular electronics applications.

Financial support from the NCCR "Nanoscale Science" is gratefully acknowledged.

## Notes and references

‡ STM images have been analyzed and processed using the freely available WSXM software.[9]

§ The molecular conformation of isolated molecules in the gas phase has been determined at the AM1 level of theory. Molecular mechanics calculations have been performed using the CHARMM22 forcefield. This forcefield has been found to correctly reproduce aromatic binding for the benzene dimer.[10] A simpler model for aromatic interactions has been developed by Hunter.[11] The nearest neighbour geometry in our work is found to be attractive also with this model.


1 C. Joachim, J. K. Gimzewski and A. Aviram, *Nature*, 2000, **408**, 541.

2 M. E. Cañas-Ventura, W. Xiao, D. Wasserfallen, K. Müllen, H. Brune, J. V. Barth and R. Fasel, *Angew. Chem., Int. Ed.*, 2007, **46**, 1814.

3 (*a*) W. Pisula, M. Kastler, D. Wasserfallen, M. Mondeshki, J. Piris, I. Schnell and K. Müllen, *Chem. Mater.*, 2006, **18**, 3634; (*b*) H. Klauk, M. Halik, U. Zschieschang, G. Schmid and W. Radlik, *J. Appl. Phys.*, 2002, **92**, 5259.

4 (*a*) J. A. Theobald, N. S. Oxtoby, M. A. Phillips, N. R. Champness and P. H. Beton, *Nature*, 2003, **424**, 1029; (*b*) R. Otero, M. Schöck, L. M. Molina, E. Laegsgaard, I. Stensgaard, B. Hammer and F. Besenbacher, *Angew. Chem., Int. Ed.*, 2005, **44**, 2270; (*c*) S. Clair, S. Pons, A. P. Seitsonen, H. Brune, K. Kern and J. V. Barth, *J. Phys. Chem. B*, 2004, **108**, 19392.

5 (*a*) S. Stepanow, M. Lingenfelder, A. Dmitriev, H. Spillmann, E. Delvigne, N. Lin, X. Deng, C. Cai, J. V. Barth and K. Kern, *Nat. Mater.*, 2004, **3**, 229; (*b*) T. Classen, G. Fratesi, G. Costantini, S. Fabris, F. L. Stadler, C. Kim, S. de Gironcoli, S. Baroni and K. Kern, *Angew. Chem., Int. Ed.*, 2005, **44**, 6142.

6 S. Xiao, M. Myers, Q. Miao, S. Sanaur, K. Pang, M. L. Steigerwald and C. Nuckolls, *Angew. Chem., Int. Ed.*, 2005, **44**, 7390.

7 (*a*) J. Lagoute, K. Kanisawa and S. Fölsch, *Phys. Rev. B: Condens. Matter Mater. Phys.*, 2004, **70**, 245415; (*b*) P. Ruffieux, O. Gröning, R. Fasel, M. Kastler, D. Wasserfallen, K. Müllen and P. Gröning, *J. Phys. Chem. B*, 2006, **110**, 11253; (*c*) L. Gross, F. Moresco, P. Ruffieux, A. Gourdon, C. Joachim and K.-H. Rieder, *Phys. Rev. B: Condens. Matter Mater. Phys.*, 2005, **71**, 165428.

8 J. L. Brédas, J. P. Calbert, D. A. da Silvo Filho and J. Cornil, *Proc. Natl. Acad. Sci. U. S. A.*, 2002, **99**, 5804.

9 I. Horcas, R. Fernandez, J. M. Gomez-Rodriguez, J. Colchero, J. Gomez-Herrero and A. M. Baro, *Rev. Sci. Instrum.*, 2007, **78**, 013705.

10 A. T. Macias and A. D. MacKerell, *J. Comput. Chem.*, 2005, **26**, 1452.

11 C. A. Hunter, *Chem. Soc. Rev.*, 1994, **23**, 101.

12 (*a*) D. Bléger, D. Kreher, F. Mathevet, A.-J. Attias, G. Schull, A. Huard, L. Douillard, C. Fiorini-Debuischert and F. Charra, *Angew. Chem., Int. Ed.*, 2007, **46**, 7404; (*b*) K. Tahara, C. A. Johnson II, T. Fujita, M. Sonoda, F. C. De Schryver, S. De Feyter, M. M. Haley and Y. Tobe, *Langmuir*, 2007, **23**, 10190.

13 (*a*) M.-C. Blüm, E. Cavar, M. Pivetta, F. Patthey and W.-D. Schneider, *Angew. Chem., Int. Ed.*, 2005, **44**, 5334; (*b*) M. Pivetta, M.-C. Blüm, F. Patthey and W.-D. Schneider, *Angew. Chem., Int. Ed.*, 2008, **47**, 1076; (*c*) V. A. Langlais, Y. Gauthier, H. Blekhir and O. Maresca, *Phys. Rev. B: Condens. Matter Mater. Phys.*, 2005, **72**, 085444.